

Supplement of Atmos. Chem. Phys., 14, 11335–11352, 2014  
<http://www.atmos-chem-phys.net/14/11335/2014/>  
doi:10.5194/acp-14-11335-2014-supplement  
© Author(s) 2014. CC Attribution 3.0 License.



*Supplement of*

**New emission factors for Australian vegetation fires measured using open-path Fourier transform infrared spectroscopy – Part 2: Australian tropical savanna fires**

**T. E. L. Smith et al.**

*Correspondence to:* T. E. L. Smith (thomas.smith@kcl.ac.uk)

## Supplementary Figures

There is a large number of data in Figure 12 (thousands of individual measurements from all of the 21 fires). There is such a large number of data for  $\text{CH}_4$  because  $\text{CH}_4$  mole fractions are retrievable from FTIR spectra even at ambient concentrations. This wealth of data provides us with samples spanning the full range of modified combustion efficiencies (from less than 80% up to almost 100 %), enabling us to calculate MCE-dependent emission ratios (as plotted in Figure 12). This is also the case for a number of other trace gases whose mole fractions in the smoke from these fires are well above the detectability limits of the spectroscopy ( $\text{CO}$ ,  $\text{C}_2\text{H}_4$ ,  $\text{CH}_2\text{O}$ ,  $\text{CH}_3\text{OH}$ ,  $\text{CH}_3\text{COOH}$ ,  $\text{NH}_3$ ). For the majority of these gases (except  $\text{C}_2\text{H}_4$ ), which are produced predominantly during smouldering-phase combustion, we see the same relationship as is evident in Figure 12 (Figure S1). For  $\text{C}_2\text{H}_4$ , which may be produced in pyrolysis as well as smouldering combustion, the relationship is not apparent (Figure S2). For gases that are close to the detectability threshold of the instrumental setup ( $\text{C}_2\text{H}_2$ ,  $\text{C}_2\text{H}_6$ ,  $\text{HCOOH}$ ,  $\text{HCN}$ ), we do not see a wealth of data, indeed, some of these gases were only detected at a few of the 21 fires (see Table 4). As such the corresponding plots for these gases are data sparse and it is not possible to draw conclusions about the relationship between MCE and emission ratios.

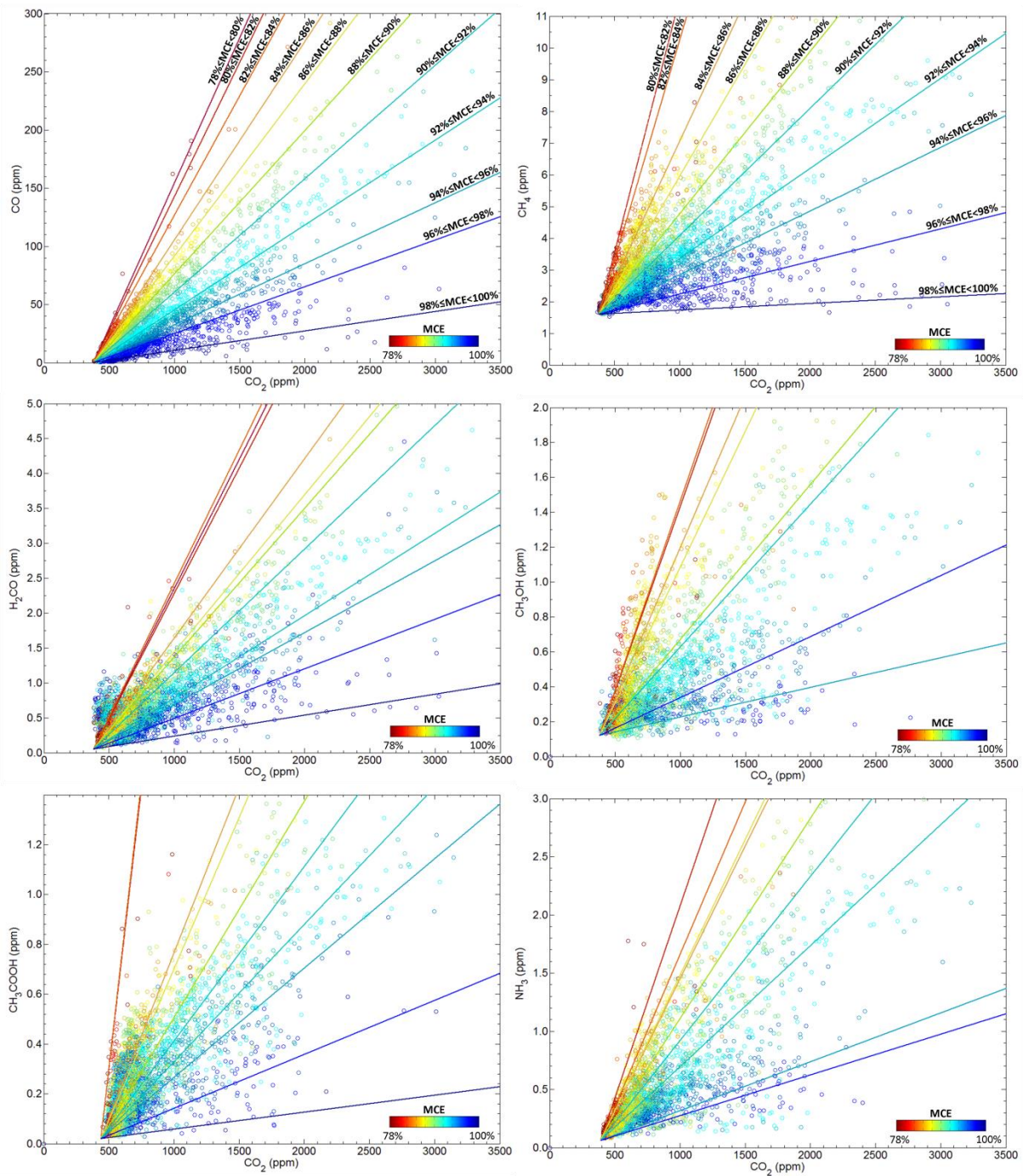


**Figure S1** Same as Figure 12, but including plots for CO, CH<sub>4</sub>, H<sub>2</sub>CO, CH<sub>3</sub>OH, CH<sub>3</sub>COOH, and NH<sub>3</sub>. Plots include all data from the 2009 and 2010 campaigns, including generalised least squares linear best-fit lines that have been calculated using measurements subsampled by narrow (2%) bins of MCE. Each line represents the line of best fit to the subsampled emissions measurements (the MCE bin for each line is indicated on the CO and CH<sub>4</sub> plots).

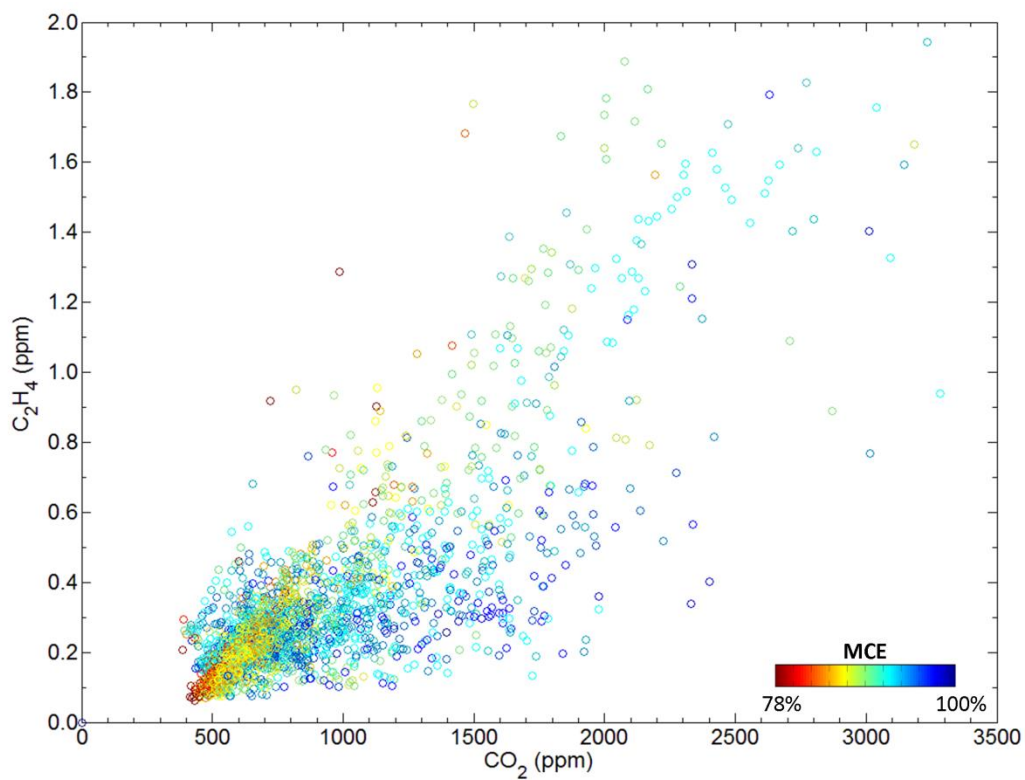


**Figure S2** Same as Figure S1, but for  $\text{C}_2\text{H}_4$ . MCE-dependent emission ratios could not be established for  $\text{C}_2\text{H}_4$ .  $\text{C}_2\text{H}_4$  emission ratios were similar, independent of MCE, probably due to production in both pyrolysis combustion (close in space and time to high-MCE flaming combustion) and smouldering combustion (low MCE).